Modification of internal temperature distribution in broad area semiconductor lasers and the effect on near- and far-field distributions

É.O'Neill, P.O'Brien, J.Houlihan and J.McInerney

Abstract: The results from two novel experimental techniques to investigate the influence of thermal effects on large aperture, high power semiconductor lasers are presented. The first technique is achieved via fabricated micro-stripe heating elements, integrated onto the laser diode using standard photolithographic technology. The second involves focusing an Ar$^+$ beam onto the injection stripe of a standard broad-area laser to investigate the effect of localised heating. Results from both experiments show that the internal temperature distribution has a pronounced influence on the near- and far-fields of large aperture semiconductor lasers. By tailoring this distribution, significant improvements to near- and far-fields can be obtained.

1 Introduction

High brightness semiconductor lasers not only require high output power but also good spatial coherence. Standard broad-area lasers suffer from poor spatial coherence and much work has focused on improving their near- and far-field distributions [1, 2]. Broad area lasers exhibit multiple linear (Hermite-Gaussian) lateral modes or, equivalently, self-stabilised non-linear modes and tend to self-focus and form filaments at high output powers [3, 4, 5]. Previous investigations have highlighted the contribution of thermal effects to the emission characteristics of these devices [6, 7, 8], however, experimental detail and analysis have been lacking. In previous work, we investigated the background temperature distribution in broad-area lasers, and measured an approximately parabolic lateral temperature profile [9]. We now demonstrate the effect of modifying the temperature distribution. By using simple resistive heating elements integrated onto the p-contact of a standard broad-area laser, we show how control of the temperature distribution can influence output brightness. In addition, we have used a high-power laser spot to investigate the effect of localised heating on the near- and far-fields. Moreover, such effects may be useful in producing beam modulation or steering. Localised heating is often caused by poor packaging, leading to solder voids between the device and the heat-sink. As such, a more detailed understanding of its effect on output characteristics is essential.

2 Micro-stripe heaters

In order to control the temperature distribution along the length of the 150 μm wide injection stripe, a 20 μm wide micro-heating element was placed along the p-contact using a photolithographic liftoff process (Fig. 1). The devices investigated were gain guided SQW-GRINSCH devices, operating at 820 nm, bonded to gold-plated copper heatsinks, and are listed in Table 1. The heating

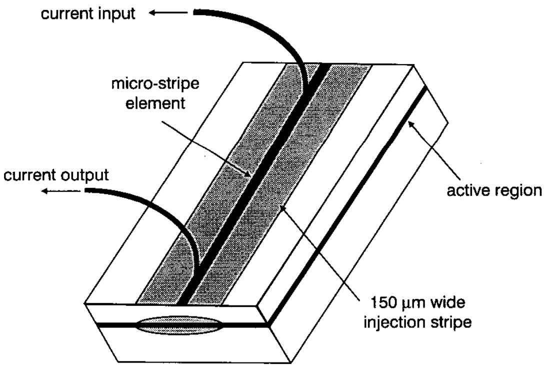

Fig. 1 *Broad area laser with micro-stripe heating elements located on the p-metallisation*

Table 1: Epitaxial structure for the SQW-GRINSCH 820 nm wafer

Material	Dopant concentration	Thickness
GaAs	Zn: $1.0{\cdot}10^{19}$ cm^{-3}	0.2 μm
GaAs	Zn: $5.0{\cdot}10^{18}$ cm^{-3}	0.2 μm
$Al_{0.60}Ga_{0.40}As$	Zn: $1.0{\cdot}10^{18}$ cm^{-3}	1.5 μm
Grade to $Al_{0.30}Ga_{0.70}As$	undoped	0.1 μm
$Al_{0.30}Ga_{0.70}As$	undoped	0.1 μm
GaAs	undoped	60 Å
$Al_{0.30}Ga_{0.70}As$	undoped	0.1 μm
Grade to $Al_{0.60}Ga_{0.40}As$	undoped	0.1 μm
$Al_{0.60}Ga_{0.40}As$	Si: $3.5{\cdot}10^{17}$ cm^{-3}	1.5 μm
GaAs	Si: $2.0{\cdot}10^{18}$ cm^{-3}	0.5 μm
GaAs substrate	Si: $1.0{\cdot}10^{18}$ cm^{-3}	500 μm

IEE Proceedings online no. 20000205
DOI: 10.1049/ip-opt:20000205
Paper first received 2nd July and in revised form 2nd December 1999

The authors are with the Optoelectronics Research Group, Department of Physics, National University of Ireland, Cork, Ireland
E-mail: scep6056@ucc.ie

element was insulated from the p-contact by a 0.2 μm Si_3N_4 layer, and connected to an external current source. The devices were bonded epitaxial side up and operated in pulsed mode (5μs/1 kHz). Current applied to the heating element produced a lattice temperature change which shifted the spontaneous emission peak wavelength (0.24 nm/°C) [9]. The spontaneous emission from the front facet was observed, and measuring the peak wavelength shift the temperature rise produced by the micro-stripe heaters was estimated. A quadratic change in peak wavelength with applied heating current was observed, thereby indicating Joule heating.

Figs. 2 and 3 show the near- and far-fields at $1.1I_{th}$. When no current is applied to the heating element, no high-intensity peaks in the near-field are visible at the position of the heating stripe. However, the application of heating current leads to the appearance of a strong peak, located at the position of the micro-heater. This effect is very pronounced in the far-field, which shows a significant improvement (the FWHM narrows from ~4° to ~2°), thereby resulting in increased brightness. The total power remains approximately constant.

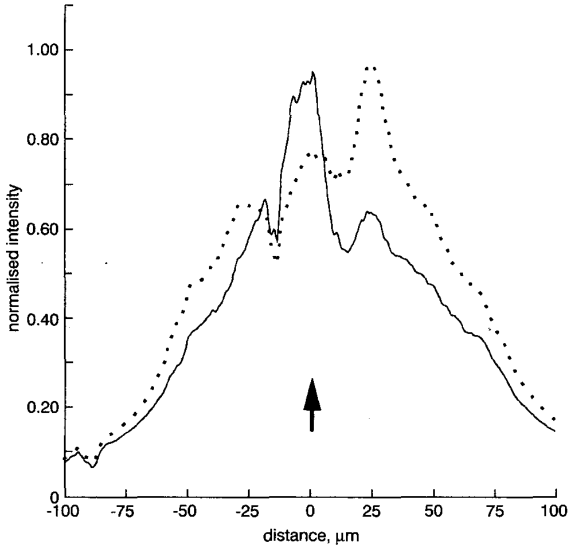

Fig. 2 *Near-field distribution at $1.1I_{th}$. The arrow indicates the position of the micro-stripe heater*
... No heating
—— 8°C heating

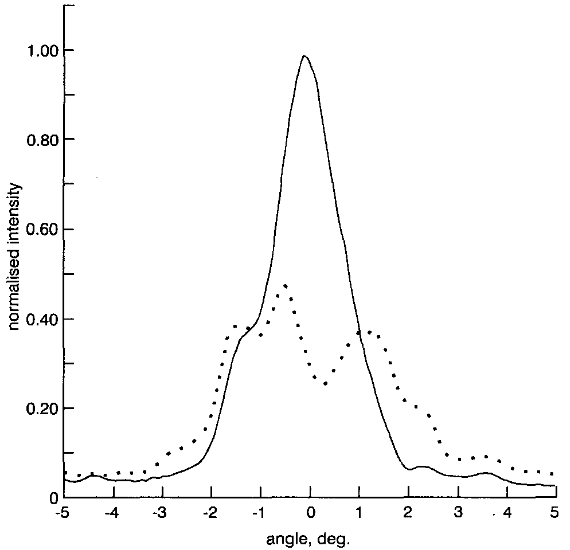

Fig. 3 *Far-field distribution at $1.1I_{th}$*
... No heating
—— 8°C heating

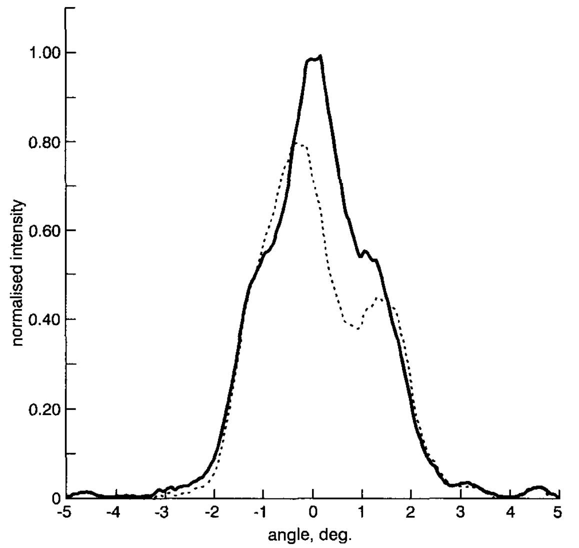

Fig. 4 *Effect of increasing the heating current on the far-field distribution at $1.5I_{th}$*
—— 8°C
... 10°C

These results suggest that heating can improve the lateral optical field distribution by forming a thermal waveguide along the length of the device. This thermal waveguide arises due to the local increase in refractive index with temperature. We found a temperature rise of ~8°C leads to the most significant improvement in the near- and far-fields. Previous work on the temperature dependence of refractive index [10], found a value of $5 \times 10^{-4} K^{-1}$ for *dn/dT* in GaAs. From our measured temperature rise we therefore estimated a corresponding local increase of ~0.12% in refractive index. Thus we see that a relatively small temperature and corresponding refractive index rise has a significant impact on the near- and far-fields. Increasing the temperature above this value we observed a deterioration in the quality of the near- and far-fields, as the improved guiding is offset by the temperature induced reduction in the local optical gain (Fig. 4). This shows competition between changes in refractive index and optical gain as we applied heating to the active region. Therefore we conclude that for low levels of heating (up to ~8°C) there is an improvement in the near- and far-field distributions leading to increased brightness. Further increases in heating causes a decrease in the output intensity.

3 Ar^+ spot heating

To investigate the effect of heating in a localised and easily controlled manner, we focused a variable power Ar^+ laser (Coherent Innova 318, λ~488 nm) onto the laser's 100 μm-wide injection stripe. The devices investigated in this section differed from those in the previous section. Again they were gain guided SQW-GRINSCH devices bonded to gold-plated copper heatsinks, however they operated at 980 nm, and are listed in Table 2. The devices were

Table 2: Epitaxial structure for the SQW-GRINSCH 980 nm wafer

Material	Dopant concentration	Thickness
GaAs	Zn: $7.0 \cdot 10^{18}\,\text{cm}^{-3}$	$0.1\,\mu m$
Grade to $Al_{0.4}Ga_{0.6}As$	Zn: $1.0 \cdot 10^{18}\,\text{cm}^{-3}$	$0.1\,\mu m$
$Al_{0.42}Ga_{0.58}As$	Zn: $1.0 \cdot 10^{18}\,\text{cm}^{-3}$	$1.2\,\mu m$
Grade to GaAs	undoped	$0.1\,\mu m$
GaAs	undoped	100 Å
$In_{0.2}Ga_{0.8}As$	undoped	70 Å
GaAs	undoped	100 Å
Grade to $Al_{0.4}Ga_{0.6}As$	undoped	$0.1\,\mu m$
$Al_{0.4}Ga_{0.6}As$	Si: $2.0 \cdot 10^{18}\,\text{cm}^{-3}$	$1.2\,\mu m$
Grade to GaAs	Si: $2.0 \cdot 10^{18}\,\text{cm}^{-3}$	$0.1\,\mu m$
GaAs	Si: $2.0 \cdot 10^{18}\,\text{cm}^{-3}$	$0.5\,\mu m$
GaAs substrate	Si: $2.0 \cdot 10^{18}\,\text{cm}^{-3}$	$500\,\mu m$

bonded epitaxial side up and operated quasi-CW ($80\,\mu s$/500 Hz). Previous work [11] has indicated that 50% of the incident power from Ar^+ laser was absorbed into the gold-chrome metallisation of the p-side contact and causes temperature rises of several degrees in the active region. There was no optical pumping from the Ar^+ spot. The Ar^+ light reflected from the metallisation was blocked using an infra-red filter. The heating spot was measured to be approximately $10\,\mu m$ FWHM and its position on the injection stripe was viewed on a CCD camera (Fig. 5). The spot was placed at various lateral and longitudinal positions on the injection stripe and the near- and far-field distributions were observed. Fig. 6 shows the positions of the three different lateral positions of the spot (at the stripe edges and centre) and Fig. 5 shows the spot in lateral position 3.

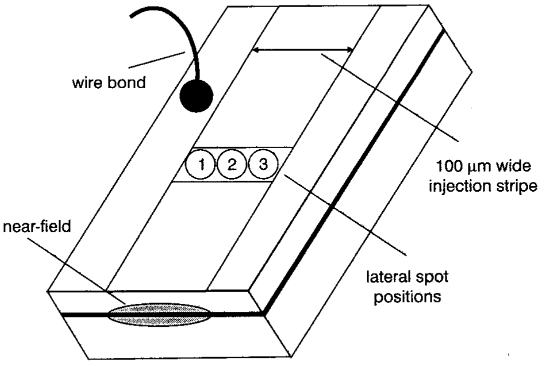

Fig. 6 *Lateral spot positions on the injection stripe for a fixed longitudinal position*

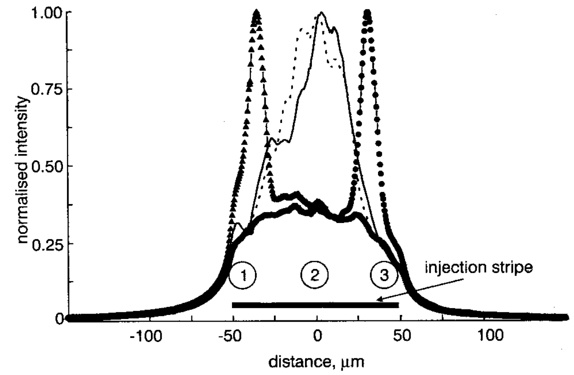

Fig. 7 *Near-field distribution at $1.1I_{th}$. (Circled numbers indicate the lateral positions of the heating spot according to Fig. 6)*

—— No spot
-▲- spot at position 1
... spot at position 2
-●- spot at position 3

3.1 Lateral positioning

We first investigated the effect of local spot heating at a fixed longitudinal position for the different lateral positions. In Fig. 7 the near-field with and without spot heating at $1.1I_{th}$ is plotted. Again, by observing the shift in the peak wavelength of the spontaneous emission, we estimated the local temperature rise due to the spot heating to be ~5°C. The pronounced positive guiding effect of the spot heating is obvious, and can be explained as follows. The spot heating is superimposed on the already present background temperature distribution. This temperature distribution, through the temperature dependence of the refractive index, produces a similarly shaped lateral refractive index profile. Thus we would expect a higher refractive index at the centre of the injection stripe than at the stripe edges. Therefore the fractional change in refractive index, produced by the spot heating, is expected to be greater at the stripe edges than at the centre. This is seen clearly in Fig. 7, where there is strong guiding at the edges of the stripe (lateral positions 1 and 3), but little effect at the centre. Fig. 8 shows the far-field distribution, with and

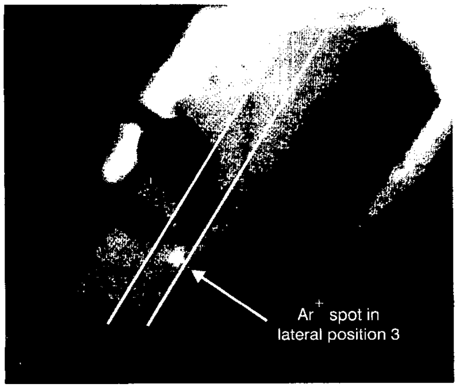

Fig. 5 *CCD image showing heating spot position the highlighted injection stripe. Detail shows the wire bond and the copper sub-mount*

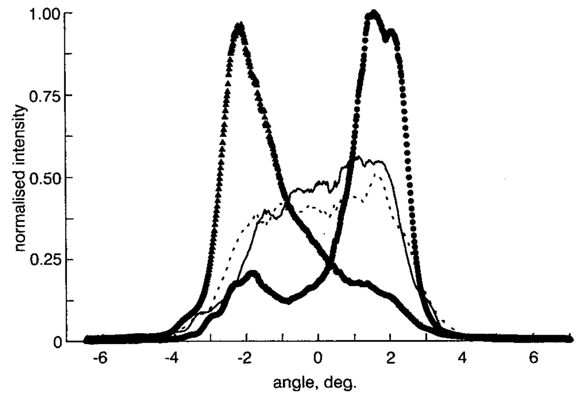

Fig. 8 *Far-field distribution at $3I_{th}$*

without spot heating, at $3I_{th}$. Again strong positive guiding can be seen when the spot is placed at the stripe edges. The intensity under all four curves in Figure 8 remains constant, indicating no significant reduction in gain at this heating level (Ar^+ power of 180 mW, local temperature rise ~5°C).

We further investigated the competition between the increase in refractive index and reduction in optical gain due to localised heating. Fig. 9 shows the near-field at $1.1I_{th}$, for different levels of spot heating power. There is strong guiding for an Ar^+ power of 180 mW, but as the Ar^+ power is further increased, the output intensity is decreased due to a reduction in optical gain. This reduction in optical gain is also apparent when we plot the peak power at $3I_{th}$ versus Ar^+ power (Fig. 10). It is important to note that at levels of Ar^+ power that produce the best guiding ($\lesssim 180$ mW) there is no significant reduction in output intensity. However, at higher levels of Ar^+ power ($\gtrsim 300$ mW) there is a significant reduction in output intensity. We have thus observed that low levels of localised heating (up to ~5°C) can have a significant impact on the near- and far-field distributions. At higher levels of heating the expected reduction in output intensity is seen.

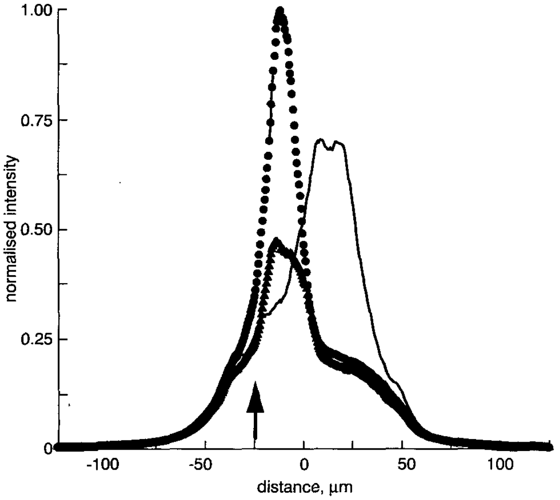

Fig. 9 *Effect of increasing localised heating on the near-field distribution at $1.1I_{th}$. The arrow indicates the position of the heating spot*

—— No spot
-●- 180 mW
-▲- 340 mW

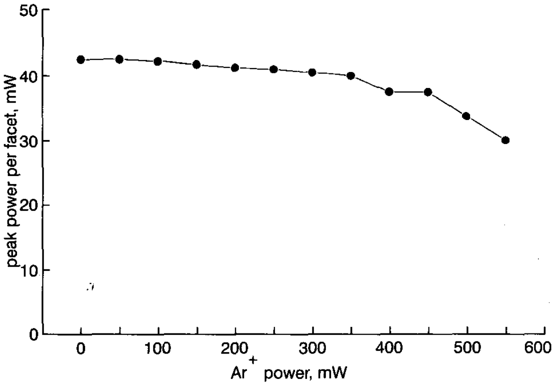

Fig. 10 *Effect of increasing the incident Ar^+ power on the output power at $3 I_{th}$*

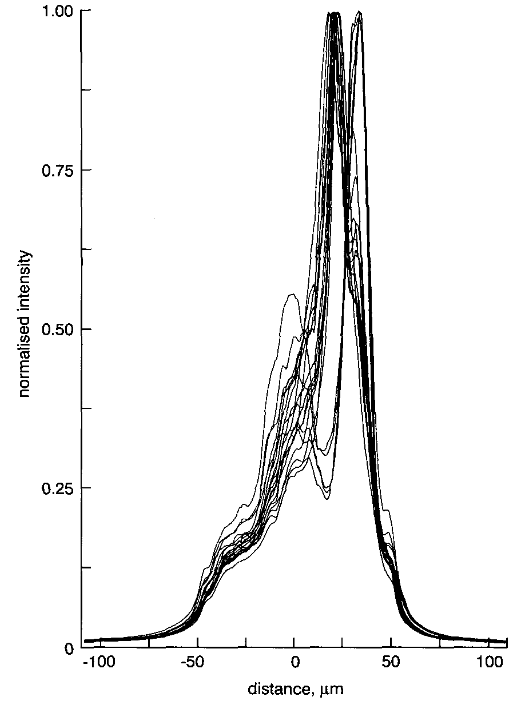

Fig. 11 *Near-field distribution at $1.1I_{th}$ for different longitudinal positions of the heating spot*

3.2 Longitudinal positioning

The effect of local spot heating at a fixed transverse position for different longitudinal positions along the entire length of the injection stripe was also investigated. In Fig. 11, with the heating spot in lateral position 3 (Fig. 6) at an Ar^+ power of 180 mW, the near-field at $1.1I_{th}$ is plotted for different longitudinal spot positions. We found the guiding effect of the spot heating to be affected very little by the longitudinal position along the stripe. It is also worth noting that the effect seen at the different lateral positions was the same regardless of longitudinal position.

4 Conclusions

We have shown that the internal temperature distribution of broad-area lasers has a very significant influence on their near- and far-fields. A simple technique for producing a thermal waveguide in order to control and improve the brightness of standard broad-area lasers has been demonstrated. In addition we have used spot heating to investigate the effect of a localised temperature increase on the near- and far-fields of these devices. In both cases we see that applied heating can have a significant effect on the output characteristics. Low level heating, if applied correctly, can improve near- and far-fields significantly while higher level heating causes a reduction in output intensity. Thus we have clearly shown that even small perturbations in the internal temperature distribution can have a pronounced effect on device performance.

5 Acknowledgments

The authors thank John Roberts at the Department of Electrical and Electronic Engineering, University of Sheffield, United Kingdom for materials growth and Mark Mullane at the Optoelectronics Research Group, Department of Physics, N.U.I., Cork, Ireland for invaluable help. This work has been supported financially by Enterprise Ireland and Optronics Ireland.

6 References

1 THOMPSON, G.H.B.: 'A theory for filamentation in semiconductor lasers including the dependence of dielectric constant on injected carrier density', *Opto-Electronics*, 1972, **4**, pp. 257–310

2 LARRSON, A., MITTELSTEIN, M., ARAKAWA, Y., and YARIV, A.: 'High-efficiency broad area single quantum well lasers with narrow single-lobed far-field patterns prepared by molecular beam epitaxy', *Electron. Lett.*, 1986, **22**, (2), pp. 79–81

3 MEHUYS, D., LANG, R.J., MITTELSTEIN, M., SALZMAN, J., and YARIV, A.: 'Self-stabilized nonlinear lateral modes of broad area lasers', *IEEE J. Quantum Electron.*, 1987, **23**, pp. 1909–1920

4 LANG, R.J., LARSSON, A.G., and CODY, J.G.: 'Lateral modes of broad area semiconductor lasers: Theory and experiments', *IEEE J. Quantum Electron.*, 1991, **27**, pp. 312–320

5 CHANG-HASNAIN, C., KAPON, E., and BHAT, R.: 'Spatial mode structure of broad-area semiconductor quantum lasers', *App. Phys. Lett.*, 1989, **54**, (3), pp. 205–207

6 HADLEY, G.R., HOHIMER, J.P., and OWYOUNG, A.: 'Comprehensive modelling of diode arrays and broad-area devices with applications to lateral index tailoring', *IEEE J. Quantum Electron.*, 1988, **24**, (11), pp. 2138–2152

7 CHEN, Y.C., REISINGER, A.R., and CHINN, S.R.: 'Thermal waveguiding in oxide-defined, narrow-stripe, large-optical-cavity lasers', *App. Phys. Lett.*, 1982, **41**, (2), pp. 129–131

8 ANDREWS, J.: 'Variable focusing due to refractive index gradients in a diode array travelling wave amplifier', *J. Appl. Phys.*, 1988, **64**, p. 2134

9 O'BRIEN, P., O'CALLAGHAN, J., and MCINERNEY, J.: 'Internal temperature distribution measurements in high power semiconductor lasers', *Electron. Lett.*, 1998, **34**, (14), pp. 1399–1401

10 MCCAULLEY, J., DONNELLY, V., VERNON, M., and TAHA, I.: 'Temperature dependence of the near infra-red refraction index of silicon, gallium arsenide and indium phosphide', *Phys. Rev. B*, 1994, **49**, (11), pp. 7408–7417

11 HOHIMER, J.P., HADLEY, G.R., and OWYOUNG, A.: 'Mode control in broad-area diode lasers by thermally induced lateral index tailoring', *App. Phys. Lett.*, 1988, **52**, (4), pp. 260–262